Acta Oncologica Vol. 32, Nos. 7/8, pp. 861–867, 1993

HIGH RESOLUTION PINHOLE SPECT FOR TUMOR IMAGING

SVEN-ERIK STRAND, MARIJANA IVANOVIC, KJELL ERLANDSSON, DAVID A. WEBER, DINKO FRANCESCHI, TERRY BUTTON and KATARINA SJÖGREEN

High-resolution, non-invasive, 3D-imaging techniques would greatly benefit the investigation of the localization properties of tumor-specific radiopharmaceuticals in laboratory animals. The present study reports how pinhole SPECT can be applied to tumor localization studies in small laboratory animals to provide high resolution SPECT images in vivo. Pinhole SPECT was performed using a rotating scintillation camera, equipped with a pinhole collimator. The sensitivity of a 2 mm diameter collimator at 45 mm from the source is 90 cps/MBq for ^{99m}Tc. The planar spatial resolution at a 45 mm distance is 2.2 mm. The transaxial spatial resolution, with a distance of 45 mm between the collimator aperture and the axis of rotation, is 3.1 mm. For SPECT imaging, spatial linearity is preserved across the usable field-of-view. The major advantage of the high resolution properties of pinhole tomography is demonstrated by the enhanced lesion-to-normal-brain uptake ratio achieved on tomographic slices as compared to planar images. For example, ^{201}Tl tumor-to-normal-brain uptake ratios of 1.1 to 1.3 observed on planar images, corresponded to ratios ranging from 3.2 to 3.7 on the SPECT slices. Examples of the activity distributions of two radiopharmaceuticals in tumor and in normal brain for sagittal and coronal images are given. In all cases, tumors are clearly delineated on the pinhole SPECT slices. The present study shows that pinhole SPECT performed with standard SPECT instrumentation can give high spatial resolution images, with a FWHM $\approx$ 3 mm and a sensitivity $\approx$ 100 cps/MBq for ^{99m}Tc.

Development of new methods for systemic radiation therapy (SRT), with tumor-specific radiopharmaceuticals, e.g. monoclonal antibodies for radioimmunotherapy (RIT), and the use of tumor-specific diagnostic agents, require high spatial resolution imaging techniques to monitor localization properties in vivo. Imaging of radiopharmaceuticals in laboratory animals is usually performed using planar scintillation camera techniques employing either a high resolution parallel hole collimator or a pinhole collimator. These techniques provide a two-dimensional representation of the three-dimensional activity distribution. The application of SPECT (single photon emission computed tomography) could provide the activity distribution in 3D. However, the spatial resolution of SPECT using parallel hole collimators is not adequate for imaging small animals. Higher resolution pinhole collimators provide the basis for performing these studies. Here we have used pinhole SPECT to investigate the comparative localization properties of several different radiopharmaceuticals, which appear to offer promise for the detection and monitoring of primary brain tumors (1–5).

A reconstruction method for cone beam tomography has been presented by Feldcamp et al. (6). Pinhole SPECT has been reported by Palmer & Wollmer for lung studies in rabbits (7). We have extended that technique for imaging the brain in rats (8).

Received 5 February 1993.
Accepted 21 August 1993.
From Radiation Physics Department, Lund University, Lund, Sweden (S.-E. Strand, K. Erlandsson, K. Sjögreen), Medical Department, Brookhaven National Laboratory (M. Ivanovic, D. A. Weber. D. Franceschi) and SUNY-SB, Stony Brook (T. Button), New York, USA.
Correspondence to: Dr Sven-Erik Strand, Radiation Physics Department, Lund University, University Hospital, S-221 85, Lund, Sweden.
Presented at the 3rd Scandinavian Symposium on Monoclonal Antibodies in Diagnosis and Therapy of Cancer, October 30–31, 1992, Helsinki Finland.

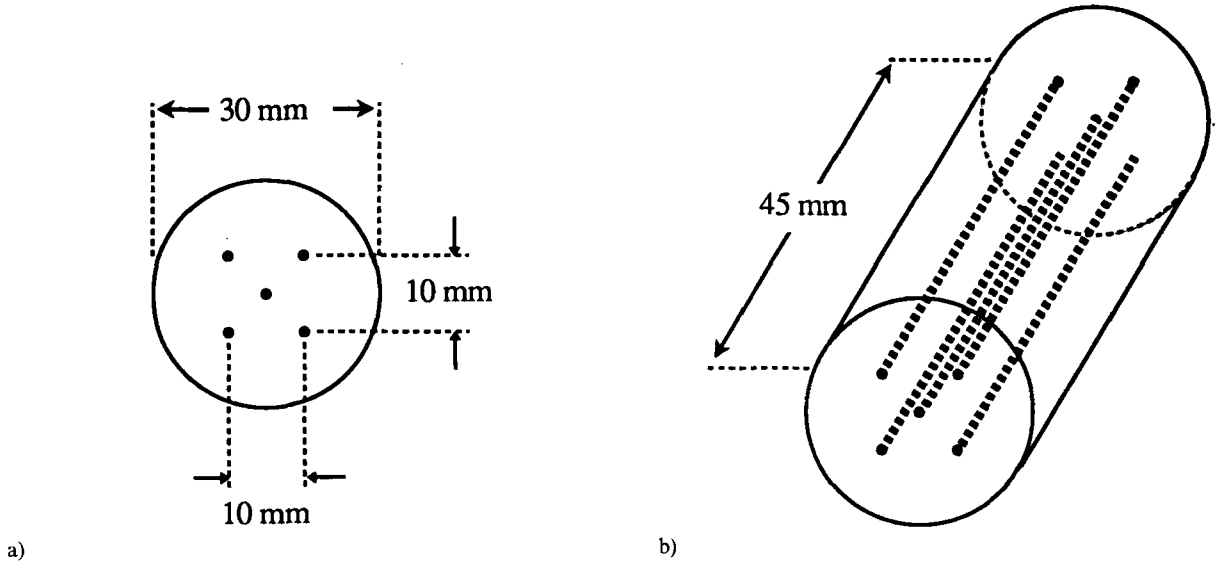

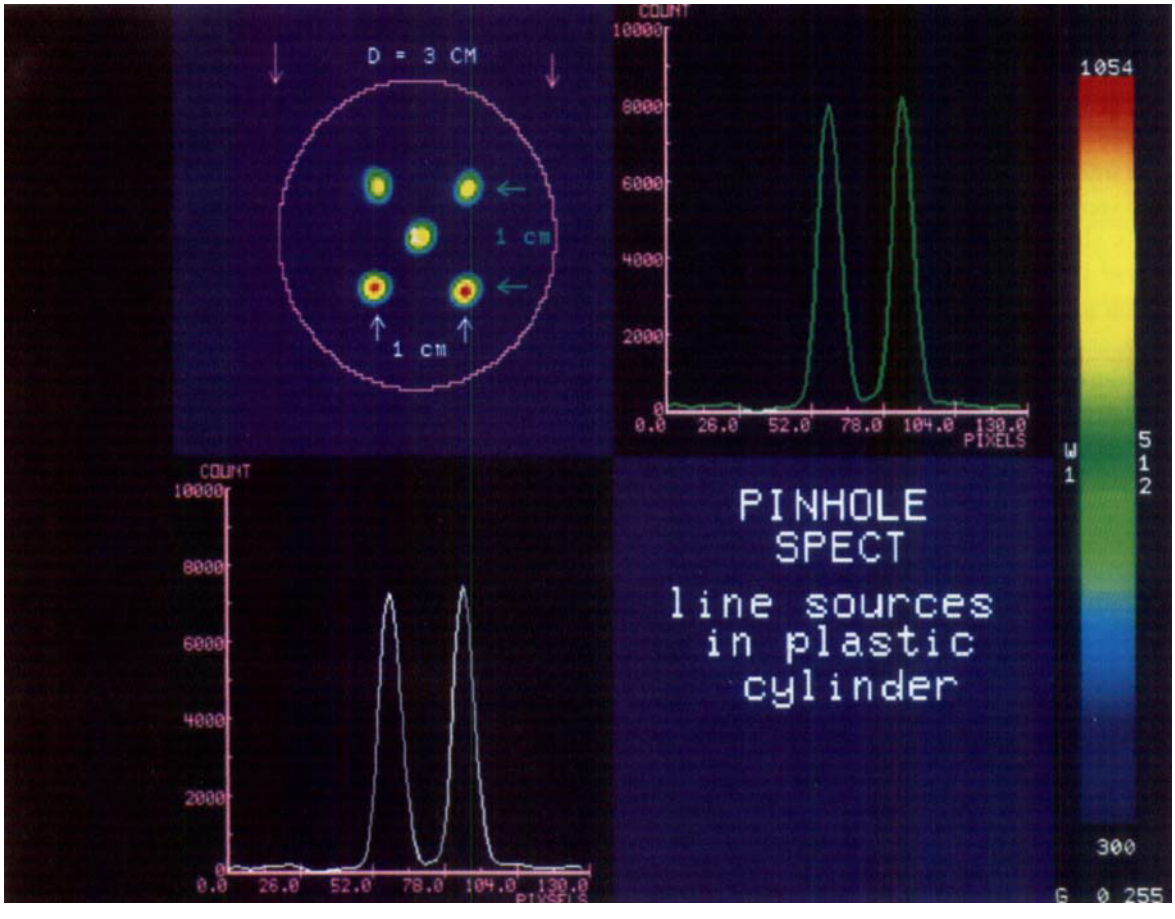

c)

Fig. 1. Test phantom with five ^{99m}Tc filled line sources (inner diameter 0.58 mm) in a plexiglass cylinder (diameter 30 mm), a–b) dimensions of the phantom, c) SPECT image and count profiles through line sources.

Material and Methods

Pinhole SPECT reconstruction. Pinhole SPECT was performed using a rotating scintillation camera (Toshiba 901A SPECT system) equipped with a 2 mm aperture pinhole collimator. The camera was rotated 360°, with projections acquired in the step-and-shoot mode. Tomographic images were reconstructed using a 3D cone-beam algorithm that is a generalization of the 2D fan-beam filtered backprojection algorithm. For the central trans-

axial plane, the two algorithms are identical. Outside this plane, the data are treated as tilted fan-beams, and the results are only approximate. A 1D reconstruction filter is applied to each fan-beam, and a weighted 3D-backprojection is used as the final step of the image reconstruction. Prior to reconstruction, the pinhole projections were corrected for the decay of the radionuclide, the geometric and intrinsic efficiency variations of the camera system, and the center-of-rotation (COR) shift. No attenuation correction was applied. A uniformity correction was made by multiplying each projection image with a normalized inverse of a flood source image. The COR shift was measured using a parallel hole collimator, and the correction was made by shifting the projections.

Imaging properties of the SPECT system. The resolution that can be achieved in pinhole SPECT is determined by the size of the pinhole aperture. Due to the magnification factor, the system spatial resolution can be better than the intrinsic resolution of the scintillation camera. The sensitivity of the system in planar mode (counts/s/MBq) was evaluated using a disc source with ^{99m}Tc (2.2 cm diameter filled with 85 MBq ^{99m}Tc in 1 ml), that was placed under the collimator at distances of 20 to 150 mm. The spatial resolution (FWHM) was obtained by imaging a line source (diameter of 1 mm and length of 80 mm) with ^{99m}Tc (48 MBq/ml). The linearity and resolution in SPECT mode was studied by imaging a cylindrical plexiglass phantom (diameter 30 mm and length 45 mm) with five line sources (inner diameter 0.58 mm and length 45 mm) 10 mm apart filled with ^{99m}Tc (see Fig. 1a). The distance between the collimator aperture and the axis of rotation was 45 mm.

Animal studies. Rats (Fischer 344) were inoculated with cultured glioma cells 2–3 weeks prior to imaging. The rats developed a tumor in the brain that was approximately 8–12 mm in diameter at the imaging time. This tumor is fast growing and the survival time of untreated animals is approximately 3 weeks (9, 10). The rats were anesthetized (ketamine/xylazine mixture) and put in a specially designed holder at the axis of rotation of the SPECT camera, which was at a distance of 45 mm from the pinhole collimator. The images were acquired in 64 × 64 matrices in zoom mode, and the total acquisition time for the SPECT study was 45 min. Examples of findings from two radiopharmaceuticals, ^{201}Tl-Cl (thallium chloride) and ^{99m}Tc-HMPAO (hexamethyl-propylen-amine-oxime) are given. The studies were carried out after the administration of 185 MBq of ^{99m}Tc-HMPAO and 37 MBq of ^{201}Tl. The radiopharmaceuticals were administered intravenously in the tail vein in a volume of 0.3–0.5 ml. MRI scans of the head of the rat were obtained in selected studies to assist in the correlation of radiopharmaceutical uptake with anatomic structures.

Results

The sensitivity of the 2 mm collimator for ^{99m}Tc is given in Fig. 2a as function of distance from the collimator. At 45 mm the sensitivity is 90 cps/MBq. The dependence of sensitivity on distance between collimator and source follows the inverse square law, as predicted by theory (11).

The spatial resolution as function of distance from the collimator aperture is given in Fig. 2b. We have also included a theoretical curve for comparison (11). The slight variations in the measured data points are due to positioning uncertainties. At 45 mm the resolution is 2.2 mm.

The results for the SPECT phantom study are given in Fig. 1c. Good spatial linearity in the system is demonstrated by the correlation of the line source spacing in the image as compared with the line source spacing in the phantom. The resolution obtained from the line sources shows a FWHM of 3.1 mm.

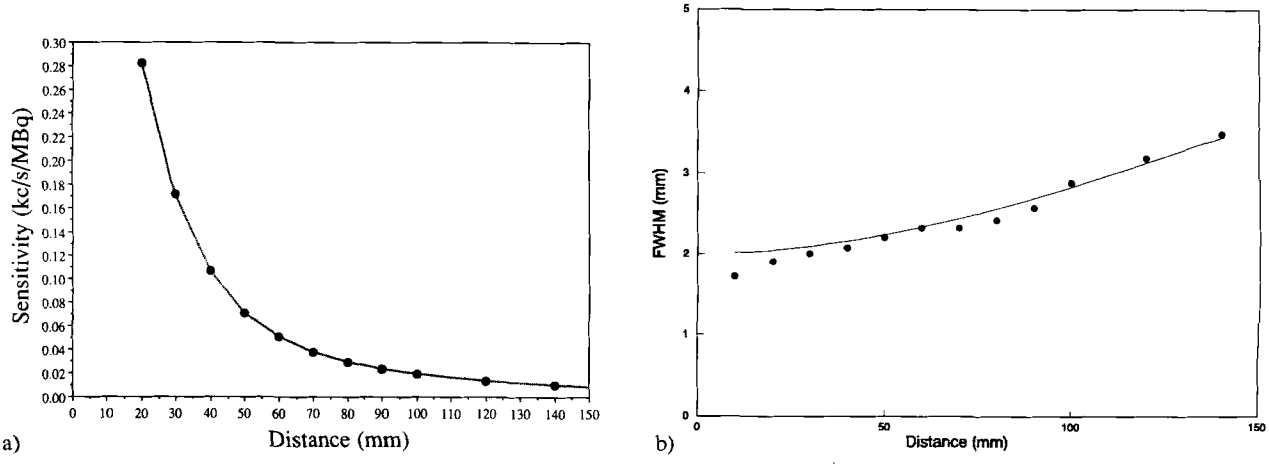

Fig. 2. Properties of the pinhole collimator (aperture 2 mm) on the large field-of-view camera for ^{99m}Tc. a) sensitivity and b) spatial resolution as function of the distance from the collimator.

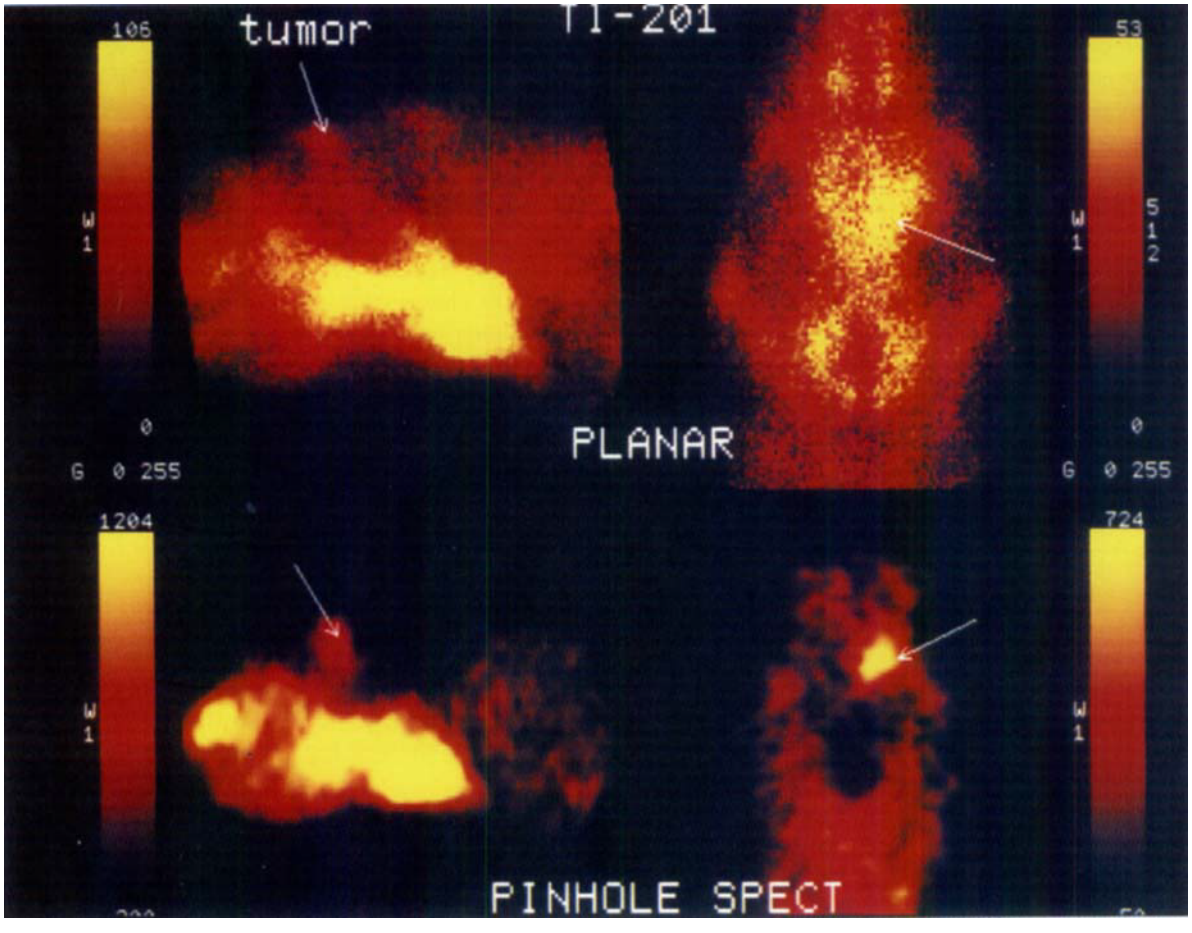

Fig. 3. ^{201}Tl images of a rat brain with tumor. Planar images: a) lateral, b) posterior; pinhole SPECT: c) sagittal d) coronal.

An example of the ^{201}Tl-Cl study in the rat's brain is given in Fig. 3. Here, both the planar and the SPECT images are given for comparison. Fig. 3a shows a left lateral planar view, and 3b the posterior planar view. Uptake in the tumor is only poorly visualized on the posterior view. Uptake ratios compared for regions of interest over the tumor to the contralateral region of the cerebellum are 1.1 and 1.2. The sagittal and coronal pinhole SPECT slices, shown in Figs 3c and d, show markedly improved contrast between the tumor and the surrounding normal brain. The corresponding contrast values are 3.7 and 3.2. This animal was not sacrificed after the measurement, and so no in vitro data are available for comparison.

An example of the corresponding ^{99m}Tc-HMPAO studies in the rat's brain is given in Fig. 4. Again, both planar and SPECT images of the localization properties of the radiopharmaceutical are shown. Fig. 4a shows the left lateral planar view, and 4b the posterior planar view. In contrast to the elevated uptake of ^{201}Tl in the tumor, a perfusion deficit in the tumor is seen with ^{99m}Tc-HMPAO. Uptake in the tumor is poorly visualized on the planar views. Uptake ratios compared for regions of interest over the tumor to the contralateral part of the cerebellum are 0.9. The sagittal and coronal pinhole SPECT slices shown in Figs 4c and d show enhanced contrast between the tumor and the surrounding brain. Corresponding uptake ratios are 0.7 and 0.8. After the measurement, the animal was sacrificed and dissected, and the activity in different organs was measured in a well-counter. The ratio between the activity concentration in the tumor and in the cerebellum was found to be 0.6.

In Fig 5, a comparison of a MRI image with the localization properties of ^{201}Tl-Cl, and ^{99m}Tc-HMPAO is shown. The tumor is well delineated on the MRI image, shows an increased uptake with ^{201}TlCl, and a reduced uptake with ^{99m}Tc-HMPAO.

Discussion

We have demonstrated that pinhole SPECT can, with a spatial resolution of about 3 mm, be used for 3D-imaging

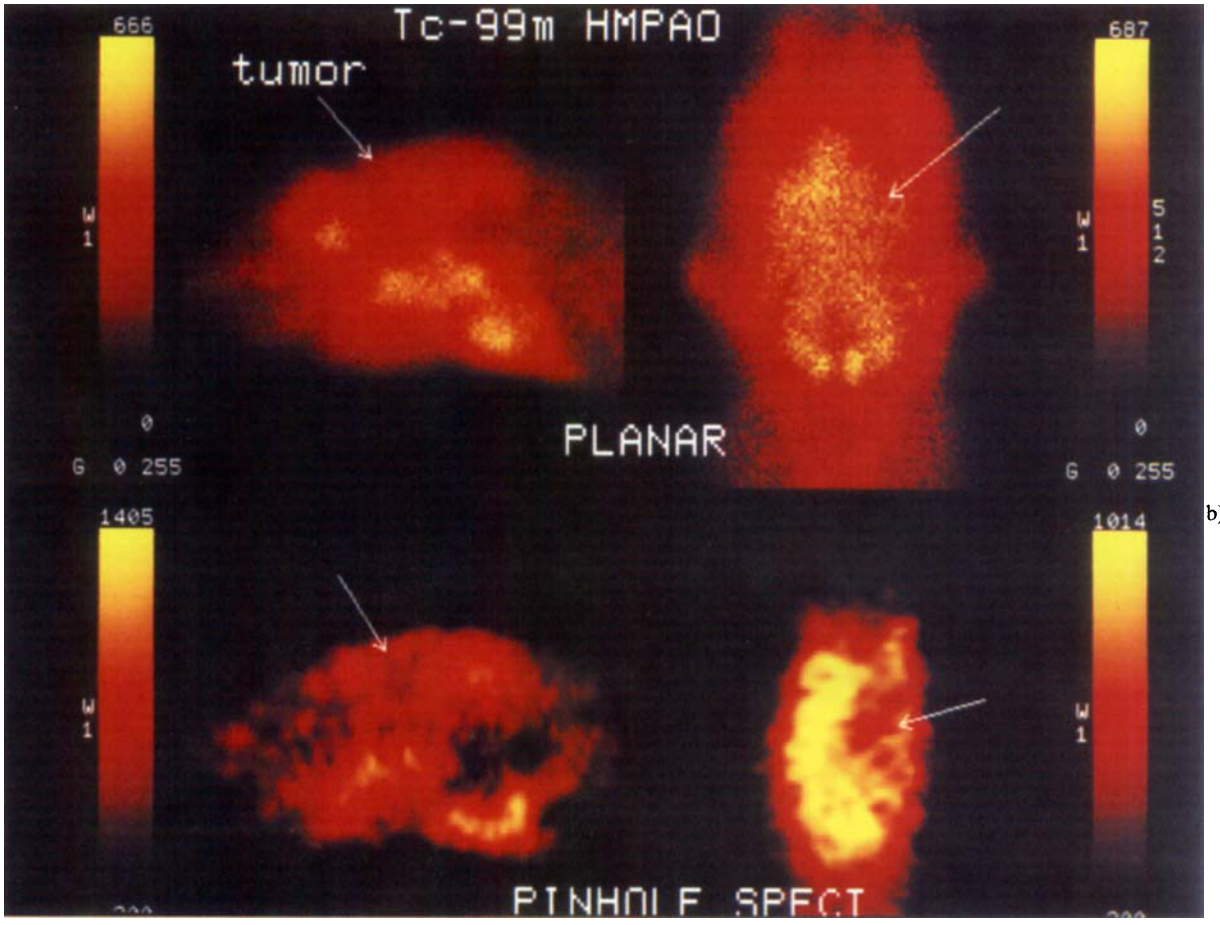

Fig. 4. ^{99m}Tc-HMPAO images of a rat brain with a tumor. Planar images: a) lateral, b) posterior; pinhole SPECT: c) sagittal d) coronal.

Table

Radioimmunotherapy radionuclides suitable for pinhole SPECT

Radionuclide	$T_{1/2}$ (d)	Decay mode	Principal energies	
			Electrons[1] keV	Photons[4] keV (%)
^{47}Sc	3.3	beta[1]	143/204	159(68)
^{67}Cu	2.6	beta	121/154/189	185(49)/93(16)
^{109}Pd	0.56	beta	361	88(3.6)
^{115m}In	0.19	beta	279	336(45)
		conv. el.[2]	308	
^{117m}Sn	13.6	conv. el.	133	158(86)
^{119}Sb	1.6	conv. el.	20	25(89)
		EC-Auger el.[3]	3	
^{123}I	0.55	conv. el.	127	159(83)
^{125}I	60.1	EC-Auger el.	4	28(139)
^{131}I	8.0	beta	192	364(81)
^{153}Sm	1.95	beta	200/226/265	70(5)/103(28)
^{165}Dy	0.1	beta	455	95(4)
^{186}Re	3.8	beta	309/362	123(2)/137(8.7)
		conv. el.	125	
^{188}Re	0.71	beta	728/794	155(15)
^{199}Au	3.1	beta	67/82/132	158(37)
^{201}Tl	3.0	EC-Auger el.	10	71(83)/167(10)

[1] Average energies for beta particles. [2] Conversion electrons. [3] Auger electrons following electron capture (EC). [4] Photons of suitable energy for scintillation camera imaging.

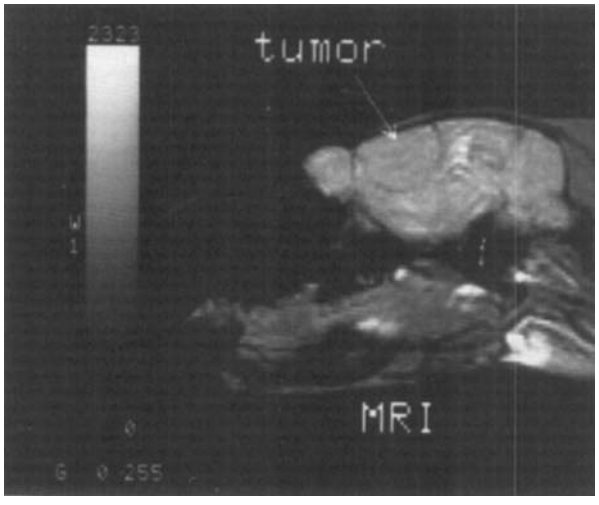

a)

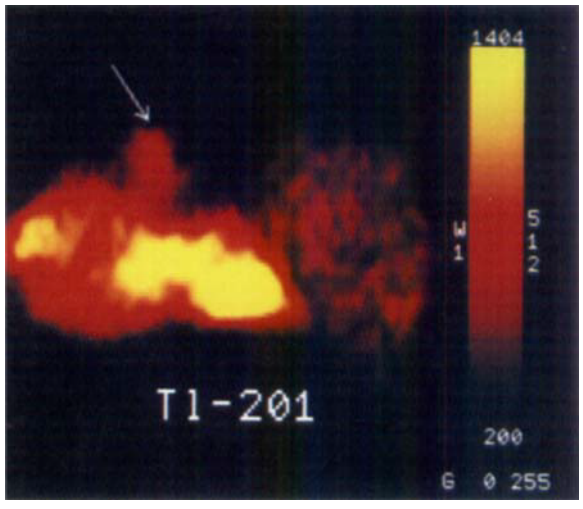

b)

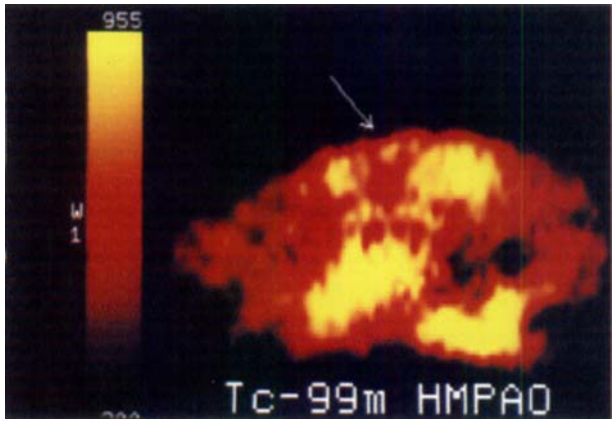

c)

Fig. 5. Comparison of a) sagittal MRI slice with b) ^{201}Tl-Cl and c) ^{99m}Tc-HMPAO pinhole SPECT slices through tumor in rats, brain. Note that in the ^{201}Tl image the tumor shows well-delineated, increased uptake whereas, in the ^{99m}Tc-HMPAO study, the tumor area is a cold spot.

studies in small animals to evaluate tumors. The resolution could be improved by using a pinhole collimator with smaller aperture at the expense of a lower sensitivity. The pinhole SPECT images show marked improvement in tumor delineation, with greatly enhanced tumor-to-normal-brain uptake ratios and significantly better definition of the localization properties of the radiopharmaceuticals throughout the brain.

Many other procedures are employed for studying the activity distribution of radiopharmaceuticals/MAbs, with spatial resolution of 1 mm or less. In vitro techniques, such as film autoradiography or beta camera studies, have shown the inhomogeneous distribution of MAb-activity in tumors (12, 13). We here demonstrate a non-invasive technique that can give a tomographic image of the activity distribution in vivo, with a spatial resolution of 3 mm or better. The technique complements other in vitro/ex vivo high resolution imaging techniques for obtaining localization data and for studying biokinetics. Many radionuclides used for experimental RIT have photon energies suitable for external imaging by this technique. Several of these are listed in the table. The present work is part of a larger study comparing localization properties and sensitivity of different radiopharmaceuticals for monitoring tumor response in external beam radiation therapy (which will be reported elsewhere).

In conclusion the present study shows that pinhole SPECT can be performed with standard SPECT instrumentation to provide high resolution images with a FWHM of about 3 mm. The sensitivity of approximately 100 cps/MBq for ^{99m}Tc is acceptable for laboratory animal studies.

ACKNOWLEDGEMENTS

This research was supported in part by U.S. DOE Contract DE-ACO2-76CH00016, the Swedish Cancer Foundation grant No. 33160-B91-01XAB, John and Augusta Persson's, Nilsson's and Mrs Berta Kamprad's Foundations, Lund, Sweden. Dr Sven-Erik Strand was also supported on sabbatical leave at Brookhaven National Laboratory by Swedish Medical Society Foundations, Royal Physiological Society and Crafoord's Foundation, Lund, Sweden.

REFERENCES

1. Kaplan WD, Takvorian T, Morris JH, Rumbaugh CL, Connolly BT, Atkins HL. Thallium-201 brain tumor imaging: A comparative study with pathologic correlation. J Nucl Med 1987; 28: 47–52.
2. Kim KT, Black KL, Marciano D, et al. Thallium-201 SPECT imaging of brain tumors: Methods and results. J Nucl Med 1990; 31: 965–7.
3. Suess E, Malessa S, Ungersback K, et al. Technetium-99m-d-I-hexamethylpropyleneamine oxime (HMPAO) uptake and glutathione content in brain tumors. J Nucl Med 1991; 32: 1675–81.
4. O'Tuama LA, Packard AB, Treves ST. SPECT imaging of pediatric brain tumor with hexakis (methoxyisobutylisonitrile) technetium (I). J Nucl Med 1990; 31: 2040–1.
5. Biersack HJ, Grunwald F, Kropp J. Single photon emission tomography imaging of brain tumors. Semin Nucl Med 1991; 21: 2–10.
6. Feldcamp LA, Davis LC, Kress JW. Practical cone-beam algorithm. J Opt Soc Am [A] 1984; 1: 612–9.
7. Palmer J, Wollmer P. Pinhole emission computed tomography: Method and experimental evaluation, Phys Med Biol 1990; 35: 339–50.
8. Strand S-E, Ivanovic M, Erlandsson K, et al. Tumor imaging with pinhole SPECT (abstract). Antibody Immunoconjugate and Radiopharmaceuticals 1992; 5: 356.
9. Joel DD, Fairchild RG, Laissue, JA, Saraf SK, Kalef-Ezra JA, Slatkin DN. Boron neutron capture therapy of intracerebral rat gliosarcomas. Proc Natl Acad Sci USA 1990; 87: 9908–12.
10. Coderre JA, Joel DD, Micca PL, Nawrocky MM, Slatkin DN. Control of intracerebral gliosarcomas in rats by boron neutron capture therapy with p-boronophenylalanine. Radiat Res 1992; 129: 290–6.
11. Anger HO. Radioisotope cameras. In: Hine GJ, ed. Instrumentation in nuclear medicine. New York: Academic Press 1967; 1.
12. Ljunggren K, Strand S-E. Beta camera for static and dynamic imaging of charged particle emitting radionuclides in biological samples. J Nucl Med 1990; 31: 2058–63.
13. Strand S-E, Ljunggren K, Kairemo K, et al. Functional imaging and dosimetric applications of the beta camera in radioimmunodiagnosis and radioimmunotherapy. Antibody Immunoconj Radiopharm 1991; 4: 631–5.